



PERGAMON

International Journal of Solids and Structures 38 (2001) 1659–1668

INTERNATIONAL JOURNAL OF  
**SOLIDS and**  
**STRUCTURES**

[www.elsevier.com/locate/ijsolstr](http://www.elsevier.com/locate/ijsolstr)

## Models of fracture of cellular monolith structures

Y.A. Antipov <sup>a,\*</sup>, A.B. Movchan <sup>b</sup>, S.T. Kolaczkowski <sup>c</sup>

<sup>a</sup> Department of Mathematical Sciences, University of Bath, Claverton Down, Bath BA2 7AY, UK

<sup>b</sup> Department of Mathematical Sciences, University of Liverpool, Liverpool L69 3BX, UK

<sup>c</sup> Department of Chemical Engineering, University of Bath, Claverton Down, Bath BA2 7AY, UK

Received 6 August 1999; in revised form 1 February 2000

---

### Abstract

This work deals with homogenization models for cracks in lattice structures representing cross-sections of catalytic monolith combustors. A simple asymptotic approach is used to describe interaction of cracks and to evaluate the stress-intensity factors. An asymptotic model of local stability of a crack interacting with a micro-defect is presented. © 2001 Elsevier Science Ltd. All rights reserved.

**Keywords:** Fracture; Cellular structures

---

### 1. Introduction

A catalytic combustor is represented by a ceramic cellular monolith structure with square, hexagonal or triangular cells. For a description of combustion reactions in a catalytic monolith, we refer to Hayes and Kolaczkowski (1997). In the present paper, we are mainly concerned with elastic fields in a damaged lattice structure. The homogenization models for cellular structures with square cells were studied by Antipov et al. (2000) with applications to propagation of cracks and crack–defect interaction. A particular feature of the lattice structure with square cells is a low resistance to shear; the homogenized material is orthotropic. In the present paper, we consider two remaining possibilities: hexagonal and triangular lattice structures. In both cases, the homogenization procedure gives isotropic media; however, the hexagonal structure is characterized by a small shear modulus (Gibson and Ashby, 1998). It is appropriate to refer to the work by Hori and Nemat-Nasser (1987) and Gong and Horii (1989) who studied numerically a long-range interaction between a finite crack and a micro-crack in 2D isotropic media. Fracture analysis of cellular materials was developed by Chen et al. (1998) in the frame of the strain gradient model. These authors analysed the asymptotic fields near the crack tip and the full-field solutions for cellular materials with hexagonal, triangular or square lattice.

We present an asymptotic algorithm that allows us to retrieve the effects similar to the ones discussed by Chen et al. (1998) and, in addition, we analyse interaction of cracks in a homogenized lattice. The structure of the integral equations, involved in the algorithm, is also similar to Rubinstein (1986). The results of the

---

\* Corresponding author. Tel.: +44-01225-826-106; fax: +44-01225-826-492.

E-mail address: [y.antipov@maths.bath.ac.uk](mailto:y.antipov@maths.bath.ac.uk) (Y.A. Antipov).

present paper are mainly analytical; the dipole fields associated with a small micro-crack were evaluated explicitly, and the asymptotic algorithm described below has the same structure as the one employed in the earlier work of Antipov et al. (2000). The main results of the present paper include the following:

- (1) asymptotic formulae for the stress-intensity factors associated with crack–defect interaction in hexagonal and triangular lattice structure;
- (2) comparison of asymptotic estimates for the stress-intensity factors for different lattice geometries;
- (3) local stability analysis in crack–defect interaction.

The structure of the paper can be described as follows: In Section 2, we give the formulation of the problem that includes governing equations, boundary conditions, characteristics of the homogenized elastic media with cracks. In Section 3, we give an explicit description of dipole fields for cracks. Section 4 includes the outline of the asymptotic algorithm used for evaluation of the stress-intensity factors. We consider the particular case of thermal load in Section 5. Section 6 presents numerical results for the stress-intensity factors and the local stability analysis for the crack–defect interaction.

## 2. Governing equations and homogenization

We consider two types of lattice structures (with hexagonal or triangular cells), where the homogenized two-dimensional elastic material is isotropic, i.e., the averaged displacement field  $\mathbf{u}$  satisfies the system of equilibrium equations

$$\mu_* \nabla^2 \mathbf{u} + (\lambda_* + \mu_*) \nabla \nabla \cdot \mathbf{u} = 0, \quad (2.1)$$

where  $\lambda_*$  and  $\mu_*$  are the 2D Lamé elastic moduli of the homogenized material. The equivalent representation of Eq. (2.1) is given by

$$\mathcal{D}^T \left( \frac{\partial}{\partial x} \right) \mathcal{H} \mathcal{D} \left( \frac{\partial}{\partial x} \right) \mathbf{u} = 0, \quad (2.2)$$

where  $\mathcal{H}$  is a  $3 \times 3$  matrix of the 2D elastic moduli of the homogenized material, and the differential operator  $\mathcal{D}$  has the form

$$\mathcal{D} \left( \frac{\partial}{\partial x} \right) = \begin{pmatrix} \frac{\partial}{\partial x_1} & 0 \\ 0 & \frac{\partial}{\partial x_2} \\ \frac{1}{\sqrt{2}} \frac{\partial}{\partial x_2} & \frac{1}{\sqrt{2}} \frac{\partial}{\partial x_1} \end{pmatrix}. \quad (2.3)$$

For triangular and hexagonal lattice structures (Fig. 1), the matrices of homogenized elastic moduli are defined as

$$\mathcal{H}^{\text{triang}} = \frac{E}{1 - \nu^2} \begin{pmatrix} \frac{3}{8}f & \frac{1}{8}f & 0 \\ \frac{1}{8}f & \frac{5}{8}f & 0 \\ 0 & 0 & \frac{1}{4}f \end{pmatrix}, \quad (2.4)$$

$$\mathcal{H}^{\text{hexag}} = \frac{E}{1 - \nu^2} \begin{pmatrix} \frac{1}{4}f + \frac{3}{8}f^3 & \frac{1}{4}f - \frac{3}{8}f^3 & 0 \\ \frac{1}{4}f - \frac{3}{8}f^3 & \frac{1}{4}f + \frac{3}{8}f^3 & 0 \\ 0 & 0 & \frac{3}{4}f^3 \end{pmatrix}, \quad (2.5)$$

where  $f$  is the area fraction of the elastic material in the 2D lattice, and  $E, \nu$  are the Young modulus and the Poisson ratio of the elastic material, respectively (derivation of Eqs. (2.4) and (2.5) is given in Kolaczkowski et al. (1999)). It follows from Eqs. (2.4) and (2.5) that the coefficients  $\lambda_*, \mu_*$  in Eq. (2.1) are

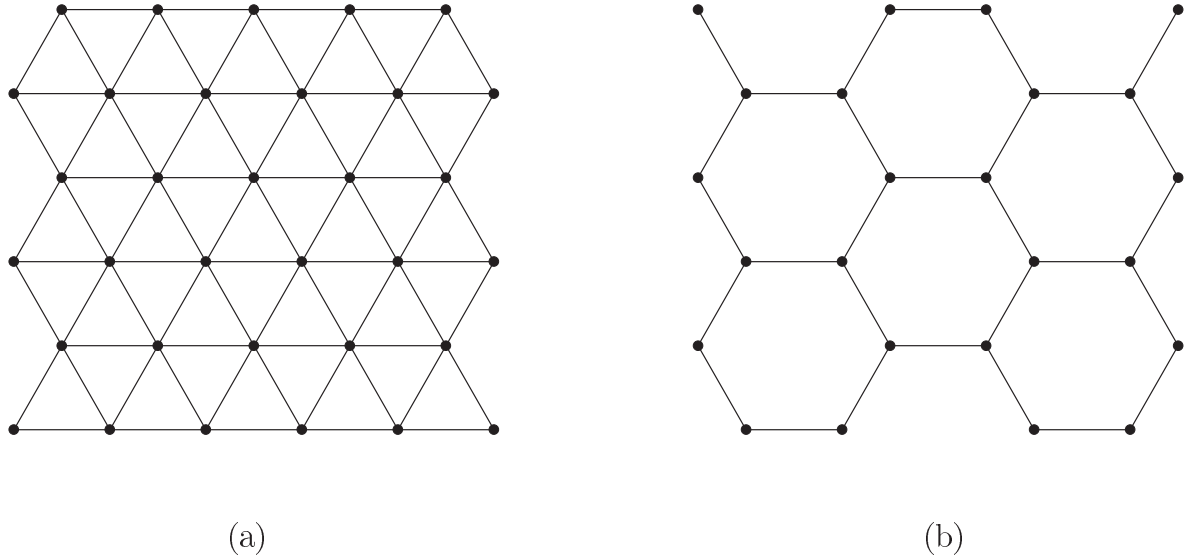


Fig. 1. Lattice structures.

$$\lambda_* = \mu_* = \frac{f}{8} \frac{E}{1 - v^2} \quad (2.6)$$

for the case of triangular lattice, and

$$\lambda_* = \frac{f}{4} \left(1 - \frac{3}{2} f^2\right) \frac{E}{1 - v^2}, \quad \mu_* = \frac{3}{8} f^3 \frac{E}{1 - v^2} \quad (2.7)$$

for hexagonal lattice structures. We remark that in three dimensions, the homogenized materials above should be treated as transversely isotropic (their elastic properties in  $(x_1, x_2)$  plane are different from those in  $(x_1, x_3)$ - and  $(x_2, x_3)$ -planes).

Let a homogenized 2D medium contain two cracks,

$$M = \{\mathbf{x} : |x_1| < a, x_2 = 0\}, \quad (2.8)$$

$$m_\varepsilon = \{\mathbf{x} : x_j = x_j^{(0)} + l_j t, j = 1, 2, |t| < \varepsilon\}, \quad (2.9)$$

where  $\varepsilon$  is a small positive non-dimensional parameter, and  $a, x_j^{(0)}, l_j$  are given constants. The crack  $M$  has a finite length  $2a$ , and the crack  $m_\varepsilon$  is small, of the length  $2\varepsilon$ ;  $\mathbf{x}^{(0)} = (x_1^{(0)}, x_2^{(0)}) = R(\cos \theta, \sin \theta)$  and  $\mathbf{l} = (l_1, l_2) = (\cos \beta, \sin \beta)$  characterize the location and orientation of the small crack. It is also assumed that  $\mathbf{x}^{(0)}$  is located at a finite distance from the crack  $M$  (i.e., the quantity  $R$  is of order  $O(1)$ ).

Traction boundary conditions are posed in the homogenized medium for the field  $\mathbf{u}$  on the crack faces  $M^\pm$  and  $m_\varepsilon^\pm$ :

$$\mathcal{D}^T(\mathbf{n}) \mathcal{H} \mathcal{D} \left( \frac{\partial}{\partial x} \right) \mathbf{u} = \mathbf{p}(\mathbf{x}) \quad \text{on } M^\pm \cup m_\varepsilon^\pm, \quad (2.10)$$

where  $\mathbf{n}$  represents the unit normal on the crack faces; the principal force and moment vectors associated with the load  $\mathbf{p}$  are assumed to be zero.

We seek the solution  $\mathbf{u}$  with a finite elastic energy. We shall evaluate the stress-intensity factors for the crack  $M$  as functions of position and orientation of the micro-crack  $m_\varepsilon$  (the stress-intensity factors also

depend, of course, on the applied load, but we deal with a model situation when the load density is constant), and analyse the local stability of the crack  $M$ .

### 3. Dipole fields for cracks

The asymptotic scheme introduced in the text below involves the so-called dipole fields for cracks. Let  $\mathcal{M}$  be a crack of the finite length  $2l$  inclined at the angle  $\beta$  to the  $x_1$ -axis. One can introduce three model fields in  $\mathbb{R}^2 \setminus \mathcal{M}$  as follows:

$$\mathbf{U}^{(j)}(\mathbf{x}) = \mathbf{V}^{(j)}(\mathbf{x}) + \mathbf{W}^{(j)}(\mathbf{x}), \quad j = 1, 2, 3, \quad (3.1)$$

which satisfy the homogeneous equilibrium equations, homogeneous traction boundary conditions and grow linearly at infinity. The fields  $\mathbf{V}^{(j)}$  are defined by

$$\mathbf{V}^{(1)}(\mathbf{x}) = \begin{pmatrix} x_1 \\ 0 \end{pmatrix}, \quad \mathbf{V}^{(2)}(\mathbf{x}) = \begin{pmatrix} 0 \\ x_2 \end{pmatrix}, \quad \mathbf{V}^{(3)}(\mathbf{x}) = \frac{1}{\sqrt{2}} \begin{pmatrix} x_2 \\ x_1 \end{pmatrix}, \quad (3.2)$$

and produce constant components of strain. Vector functions  $\mathbf{W}^{(j)}$ ,  $j = 1, 2, 3$ , are assumed to decay at infinity, and they compensate for the discrepancy left by  $\mathbf{V}^{(j)}$  in the traction boundary conditions on the crack faces;  $\mathbf{W}^{(j)}$  are called the dipole fields of the crack  $\mathcal{M}$ . At infinity,  $\mathbf{W}^{(j)}$  have the following asymptotic representation:

$$\mathbf{W}^{(j)} = \sum_{j=1}^3 P_{jk} \left( \mathbf{V}^{(j)} \left( \frac{\partial}{\partial \mathbf{x}} \right) \right)^T \mathbf{T}(\mathbf{x}) + \mathcal{O} \left( \frac{1}{\|\mathbf{x}\|^2} \right), \quad (3.3)$$

where  $\mathbf{V}^{(j)}(\partial/\partial \mathbf{x})$  are the vector differential operators defined by Eq. (3.2) ( $x_j$  should be replaced by  $\partial/\partial x_j$ ),  $\mathbf{T}(\mathbf{x})$  is Green's tensor for 2D elasticity. The matrix  $\|P_{jk}\|_{j,k=1}^3$  is called the dipole matrix of the crack; it is symmetric, negative definite. Explicit representation of the matrix  $\mathbf{P}$  (Movchan and Serkov, 1997) is given by

$$\mathbf{P} = -\frac{\pi l^2(\lambda + 2\mu)}{4\mu} \begin{pmatrix} \Xi + \Omega + \Sigma & \Xi - \Omega & \Lambda \\ \Xi - \Omega & \Xi + \Omega - \Sigma & \Lambda \\ \Lambda & \Lambda & 2\Theta \end{pmatrix}, \quad (3.4)$$

where

$$\Omega = \frac{2\mu^2}{\lambda + \mu}, \quad \Xi = 2(\lambda + \mu), \quad \Sigma = -4\mu \cos 2\beta, \quad \Lambda = -2\sqrt{2}\mu \sin 2\beta, \quad \Theta = \mu,$$

and  $\lambda, \mu$  are the 2D elastic moduli of the material (compare with Eq. (2.1)).

It is straightforward to evaluate the stress components associated with the dipole fields. Assume, for simplicity, that the crack faces are subjected to constant normal and tangential tractions

$$\sigma_{nn} = -p_2^0, \quad \sigma_{ns} = -p_1^0 \quad (3.5)$$

on the crack boundary. Then, it follows from Eqs. (3.3) and (3.4) that the stress components are characterized by the following asymptotics:

$$\sigma(\xi_1, \xi_2) = \Sigma(\xi_1, \xi_2) + \mathcal{O}(r^{-3}), \quad r \rightarrow \infty, \quad (3.6)$$

$$\Sigma_{11}(\xi_1, \xi_2) = \frac{l^2}{2r^2} [-\sin 2\alpha(2 \cos 2\alpha + 1)p_1^0 + (2 \cos^2 2\alpha - 1)p_2^0],$$

$$\Sigma_{12}(\xi_1, \xi_2) = \frac{l^2}{2r^2} [(2 \cos^2 2\alpha - 1)p_1^0 + \sin 2\alpha(2 \cos 2\alpha - 1)p_2^0],$$

$$\Sigma_{22}(\xi_1, \xi_2) = \frac{l^2}{2r^2} [\sin 2\alpha(2 \cos 2\alpha - 1)p_1^0 + (-2 \cos^2 2\alpha + 2 \cos 2\alpha + 1)p_2^0], \quad (3.7)$$

where polar coordinates  $(r, \alpha)$  and the components  $\Sigma_{ij}(\xi_1, \xi_2)$  are associated with the local system coordinates  $(\xi_1, \xi_2)$  (the  $\xi_1$ -axis is aligned along  $\mathcal{M}$ ), and

$$r = \sqrt{\xi_1^2 + \xi_2^2}, \quad \sin 2\alpha = \frac{2\xi_1 \xi_2}{r^2}, \quad \cos 2\alpha = \frac{\xi_1^2 - \xi_2^2}{r^2}.$$

#### 4. The asymptotic algorithm

The asymptotic approximation of the displacement field  $\mathbf{u}$  is sought in the form

$$\mathbf{u}(\mathbf{x}, \varepsilon, f) \sim \mathbf{v}(\mathbf{x}, f) + \varepsilon \mathbf{w}(\xi, f) + \varepsilon^2 \mathbf{q}(\mathbf{x}, f), \quad (4.1)$$

where  $\zeta = \varepsilon^{-1}(\mathbf{x} - \mathbf{x}^{(0)})$  defines stretched coordinates introduced in a neighbourhood of the small crack  $m_e$ ;  $f$  is a small area fraction of material in a 2D lattice;  $\varepsilon$  is a non-dimensional small parameter characterizing the length of  $m_e$ . Here we assume that  $\varepsilon \ll f$ .

(1) The vector function  $\mathbf{v}$  represents the displacement field in  $\mathbb{R}^2 \setminus M$ . It satisfies the system of equilibrium equations (the micro-crack  $m_e$  is absent). The representation for the field  $\mathbf{v}$  is well-known (Sedov, 1972). The stress components evaluated at  $(x_1^{(0)}, x_2^{(0)})$  admit the integral representations:

$$\begin{aligned} \sigma_{11}^0 &= \frac{1}{\pi} \int_{-a}^a \phi_1(\xi) \frac{x_2[3(x_1 - \xi)^2 + x_2^2]}{[(x_1 - \xi)^2 + x_2^2]^2} d\xi - \frac{1}{\pi} \int_{-a}^a \phi_2(\xi) \frac{(x_1 - \xi)[(x_1 - \xi)^2 - x_2^2]}{[(x_1 - \xi)^2 + x_2^2]^2} d\xi, \\ \sigma_{12}^0 &= -\frac{1}{\pi} \int_{-a}^a \phi_1(\xi) \frac{(x_1 - \xi)[(x_1 - \xi)^2 - x_2^2]}{[(x_1 - \xi)^2 + x_2^2]^2} d\xi + \frac{1}{\pi} \int_{-a}^a \phi_2(\xi) \frac{x_2[-(x_1 - \xi)^2 + x_2^2]}{[(x_1 - \xi)^2 + x_2^2]^2} d\xi, \\ \sigma_{22}^0 &= \frac{1}{\pi} \int_{-a}^a \phi_1(\xi) \frac{x_2[-(x_1 - \xi)^2 + x_2^2]}{[(x_1 - \xi)^2 + x_2^2]^2} d\xi - \frac{1}{\pi} \int_{-a}^a \phi_2(\xi) \frac{(x_1 - \xi)[(x_1 - \xi)^2 + 3x_2^2]}{[(x_1 - \xi)^2 + x_2^2]^2} d\xi, \end{aligned} \quad (4.2)$$

where  $x_1 = x_1^{(0)}$ ,  $x_2 = x_2^{(0)}$ ,

$$\phi_j(\xi) = \frac{1}{\pi \sqrt{a^2 - \xi^2}} \int_{-a}^a \frac{\sqrt{a^2 - \tau^2} p_j(\tau)}{\tau - \xi} d\tau, \quad (4.3)$$

and  $p_1, p_2$  are the components of the tractions applied on  $M^\pm$  (see Eq. (2.10)).

(2) The vector field  $\mathbf{v}$  does not necessarily satisfy the traction boundary conditions (2.10) on  $m_e$ , and the error is to be removed by the boundary layer  $\varepsilon \mathbf{w}(\xi, f)$ . Let  $m = \varepsilon^{-1} m_e$ . The vector function  $\mathbf{w}$  satisfies the homogeneous equilibrium equations (2.1) (with  $\mathbf{x}$  being replaced by  $\zeta$ ), and the traction boundary conditions on the faces of the scaled crack  $m$ :

$$-\sin \beta \begin{pmatrix} \sigma_{11}(\mathbf{w}; \zeta) \\ \sigma_{12}(\mathbf{w}; \zeta) \end{pmatrix} + \cos \beta \begin{pmatrix} \sigma_{12}(\mathbf{w}; \zeta) \\ \sigma_{22}(\mathbf{w}; \zeta) \end{pmatrix} = \mathbf{p}^{(1)}, \quad (4.4)$$

where

$$\mathbf{p}^{(1)} = \mathbf{p} + \sin \beta \begin{pmatrix} \sigma_{11}(\mathbf{v}; \mathbf{x}^{(0)}) \\ \sigma_{12}(\mathbf{v}; \mathbf{x}^{(0)}) \end{pmatrix} - \cos \beta \begin{pmatrix} \sigma_{12}(\mathbf{v}; \mathbf{x}^{(0)}) \\ \sigma_{22}(\mathbf{v}; \mathbf{x}^{(0)}) \end{pmatrix}. \quad (4.5)$$

The solution  $\mathbf{w}$  is sought in the class of functions which decay at infinity (we note that the right-hand side of Eq. (4.4) is self-balanced, i.e. its principal force and moment vectors are equal to zero). The functions  $p_1^0$ ,  $p_2^0$  that are involved in the boundary conditions (3.5) are expressed through quantities (4.2) as follows:

$$\begin{aligned} p_1^0 &= p_1 - \frac{\sin 2\beta}{2} (\sigma_{11}^0 - \sigma_{22}^0) + \cos 2\beta \sigma_{12}^0, \\ p_2^0 &= p_2 + \sin^2 \beta \sigma_{11}^0 + \cos^2 \beta \sigma_{22}^0 - \sin 2\beta \sigma_{12}^0. \end{aligned} \quad (4.6)$$

The asymptotic representation at infinity involves the dipole matrix  $\mathbf{P}$  defined in Eq. (3.4); the stress components are given by asymptotic formulae (3.6) and (3.7), where  $r$  should be replaced by  $|\zeta|$ .

(3) The field  $\varepsilon\mathbf{w}(\zeta; f)$  produces an error of order  $\mathcal{O}(\varepsilon^2)$  in the traction boundary conditions on the faces  $M^\pm$  of the crack  $M$ . Here, at the third step of the algorithm we introduce the function  $\varepsilon^2\mathbf{q}$ , which satisfies the equilibrium system (2.1) in  $\mathbb{R}^2 \setminus M$  and the following boundary conditions on  $M^\pm$ :

$$\sigma_{j2}(\mathbf{q}) = -F_j(x_1), \quad -a < x_1 < a \quad (j = 1, 2), \quad (4.7)$$

where the right-hand side is defined through the first term in Eq. (3.6), namely

$$\begin{aligned} F_1(x_1) &= \frac{1}{2} \sin 2\beta [\Sigma_{11}(x'_1, x'_2) - \Sigma_{22}(x'_1, x'_2)] + \cos 2\beta \Sigma_{12}(x'_1, x'_2), \\ F_2(x_1) &= \sin^2 \beta \Sigma_{11}(x'_1, x'_2) + \cos^2 \beta \Sigma_{22}(x'_1, x'_2) + \sin 2\beta \Sigma_{12}(x'_1, x'_2), \end{aligned} \quad (4.8)$$

where

$$x'_1 = \cos \beta (x_1 - x_1^{(0)}) - \sin \beta x_2^{(0)}, \quad x'_2 = -\sin \beta (x_1 - x_1^{(0)}) - \cos \beta x_2^{(0)}.$$

(4) The stress-intensity factors  $K_j^\pm$  characterizing singular stress fields in the vicinity of the end points  $(\pm a, 0)$  of the crack  $M$  can be evaluated as follows:

$$K_j^\pm = K_j^\pm(\mathbf{v}) + \varepsilon^2 K_j^\pm(\mathbf{q}) + \mathcal{O}(\varepsilon^3), \quad j = \text{I, II}. \quad (4.9)$$

Here,

$$\begin{aligned} K_{\text{I}}^\pm(\mathbf{q}) &= -\frac{1}{\sqrt{\pi a}} \int_{-a}^a \sigma_{22}(\mathbf{q}) \left( \frac{a+t}{a-t} \right)^{\pm 1/2} dt, \\ K_{\text{II}}^\pm(\mathbf{q}) &= -\frac{1}{\sqrt{\pi a}} \int_{-a}^a \sigma_{12}(\mathbf{q}) \left( \frac{a+t}{a-t} \right)^{\pm 1/2} dt. \end{aligned} \quad (4.10)$$

As  $x_1 \rightarrow \pm a \pm 0$  and  $x_2 = 0$ , the traction components  $\sigma_{12}, \sigma_{22}$  are characterized by the asymptotic formulae

$$\begin{aligned} \sigma_{12} &= \frac{K_{\text{II}}^\pm}{\sqrt{2\pi|x_1 \mp a|}} + \mathcal{O}(1), \\ \sigma_{22} &= \frac{K_{\text{I}}^\pm}{\sqrt{2\pi|x_1 \mp a|}} + \mathcal{O}(1). \end{aligned} \quad (4.11)$$

**Remark.** If  $M$  is a semi-infinite crack, i.e.

$$M = \{\mathbf{x} : x_2 = 0, x_1 < l\},$$

then one can also use the results of Movchan et al. (1991) and Valentini et al. (1999) to evaluate the perturbation of the crack trajectory due to interaction with the micro-crack  $m_e$ . Then it is appropriate to replace  $M$  by

$$M_\varepsilon = \{\mathbf{x} : x_2 = \varepsilon^2 h(x_1), x_1 < l\},$$

where the function  $h$  is chosen in such a way that the stress-intensity factor  $K_{II}$  (evaluated to order  $O(\varepsilon^2)$ ) at the end of  $M_\varepsilon$  is equal to zero. It means that  $M_\varepsilon$  “propagates” in an elastic plane with a small defect (micro-crack) being a Mode-I crack. Both, the dipole field contribution given by Eq. (4.9) and the crack deflection (see the classical article by Cotterell and Rice (1980)) contribute to the final answer for the stress-intensity factors. The crack deflection  $\varepsilon^2 h$  (we refer to Valentini et al. (1999)) is proved to be independent of the effective elastic moduli  $\lambda_*$ ,  $\mu_*$ , and it is given by

$$\begin{aligned} \varepsilon^2 h(l) &= \frac{\varepsilon^2}{8x_2^{(0)}} \left\{ 4 - z \left[ 3 + 2z - z^2 + 2 \cos 2\beta(1+2z)(1-z^2) - 2 \sin 2\beta(2z-1)(1+z)\sqrt{1-z^2} \right] \right\}, \\ z &= \frac{x_1^{(0)} - l}{\sqrt{(x_2^{(0)})^2 + (x_1^{(0)} - l)^2}}. \end{aligned} \quad (4.12)$$

We note that the crack deflection has the same form in homogenized media corresponding to lattice structure both with triangular and hexagonal cells (see Eqs. (2.4) and (2.5)). Also, the deflection of infinity (as  $l \rightarrow +\infty$ ) does not depend on the orientation of the micro-crack  $m_\varepsilon$ . The crack deflection formula (4.12) differs from the one derived for the case of the rectangular lattice (see formula (7.12) in Antipov et al. (2000)). In particular, we remark that the homogenized material with rectangular cells is orthotropic and has low resistance to shear, the crack trajectory changes, as  $l \rightarrow +\infty$ , for different orientations of the micro-crack  $m_\varepsilon$ .

## 5. Interaction of a finite crack and a micro-crack in a lattice under thermal load

It is natural to assume that the cellular structure of catalytic combustor monoliths is subjected to a temperature load. Let  $\alpha_T$  denote the coefficient of thermal expansion, and also assume that ideal thermal contact (continuity of temperature and the heat flux) is maintained on the crack faces. We consider the interaction of two cracks  $M$  and  $m_\varepsilon$  (Section 2); the right-hand side in the boundary condition (2.10) has the form

$$\mathbf{p} = (2\mu_* + 3\lambda_*)\alpha_T T \mathbf{n}. \quad (5.1)$$

In particular, for a hexagonal lattice,

$$\mathbf{p} = \mathbf{p}^{\text{hexag}} = \frac{3E}{4(1-\nu^2)} \left( f - \frac{1}{2}f^3 \right) \alpha_T T \mathbf{n}, \quad (5.2)$$

and for a triangular lattice

$$\mathbf{p} = \mathbf{p}^{\text{triang}} = \frac{5E}{8(1-\nu^2)} f \alpha_T T \mathbf{n}. \quad (5.3)$$

For the sake of simplicity we assume that the temperature distribution is uniform. In the asymptotic scheme described in Section 4, the field  $\mathbf{v}$  can be defined via the Westergaard potential

$$Z_1 = \frac{z}{\sqrt{z^2 - a^2}} - 1, \quad (5.4)$$

where  $z = x_1 + ix_2$ . Then, the stress components  $\sigma_{ij}(\mathbf{v})$  are given by (Sedov, 1972)

$$\begin{aligned}
\sigma_{11}(\mathbf{v}) &= p[\operatorname{Re} Z_I(z) - x_2 \operatorname{Im} Z_I(z)], \\
\sigma_{12}(\mathbf{v}) &= -px_2 \operatorname{Re} Z'_I(z), \\
\sigma_{22}(\mathbf{v}) &= p[\operatorname{Re} Z_I(z) + x_2 \operatorname{Im} Z'_I(z)]. \tag{5.5}
\end{aligned}$$

The boundary layer  $\varepsilon \mathbf{w}(\zeta, f)$  (it is the second term in Eq. (4.1)) satisfies the homogeneous equilibrium system (2.1) in  $\mathbb{R}^2 \setminus m$ ,  $m = \varepsilon^{-1} m_\varepsilon$ , and the traction boundary conditions (4.4), where  $p$  should be replaced by Eq. (5.2) for a hexagonal lattice or by Eq. (5.3) for a triangular lattice. The stress-intensity factors  $K_j^\pm$  for the crack  $M$  are determined by Eq. (4.9), where

$$K_{\text{II}}^\pm(\mathbf{v}) = 0, \quad K_I^\pm(\mathbf{v}) = p\sqrt{\pi a}, \quad p = \|\mathbf{p}\|$$

with  $\mathbf{p}$  being defined by the Eqs. (5.2) and (5.3). The perturbation terms are given by Eqs. (4.7) and (4.10) and they depend on the applied temperature  $T$ , position and orientation of the micro-crack  $m_\varepsilon$ . The answers for the hexagonal and triangular lattices differ just by a scalar factor.

In the following section, we present evaluation of the stress-intensity factors for different positions and orientations of the micro-crack and study the local stability of the crack  $M$ .

## 6. Numerical examples: evaluation of the stress-intensity factors, and the local stability analysis

The asymptotic solutions derived in the text above is used to evaluate the stress-intensity factors and to study the local stability of the large crack  $M$ .

In Fig. 2, we show the perturbation terms in the representations of the normalized stress-intensity factors, and these graphs, periodic in  $\beta$ , show that the sign of the perturbation terms depends on the orientation and position of the micro-crack  $m_\varepsilon$ . For completeness, we also present the graphs of the perturbation terms when  $\beta$  is fixed and  $\theta$  is varying (Fig. 3). In Figs. 2 and 3, we used the normalization of the stress-intensity factors of the form  $K_j^\pm/C$ ,  $j = \text{I}, \text{II}$ , where the constant  $C$  depends on the type of the lattice. In particular, for the triangular lattice,

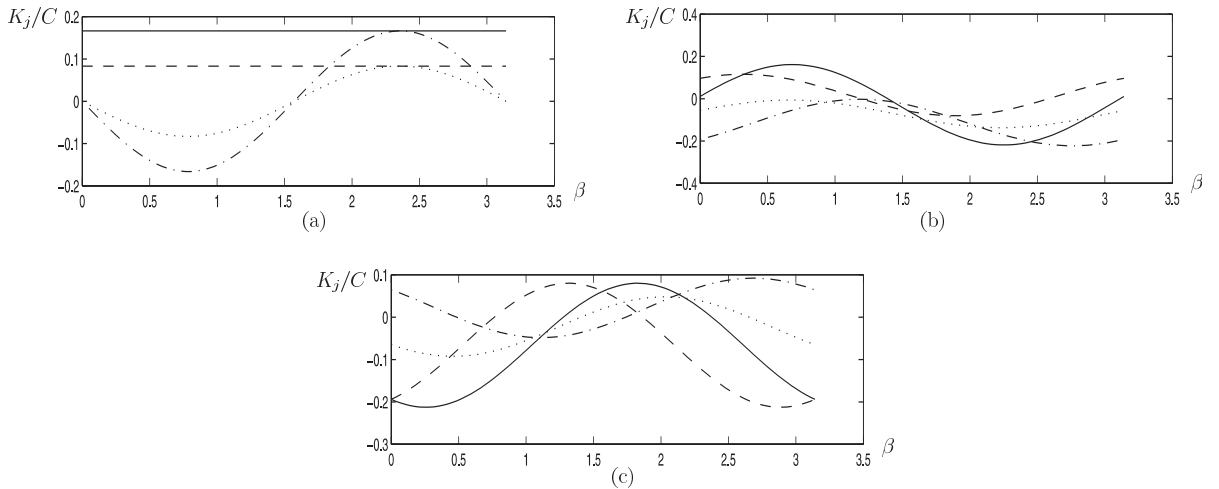


Fig. 2. Perturbation of the normalized stress-intensity factors  $C^{-1} K_j^\pm$  versus  $\beta$ . (—)  $C^{-1} K_I^+$ , (---)  $C^{-1} K_I^-$ , (· · ·)  $C^{-1} K_{II}^+$ , (· · ·)  $C^{-1} K_{II}^-$ ; (a)  $\theta = 0$ , (b)  $\theta = \pi/4$ , and (c)  $\theta = \pi/2$ .

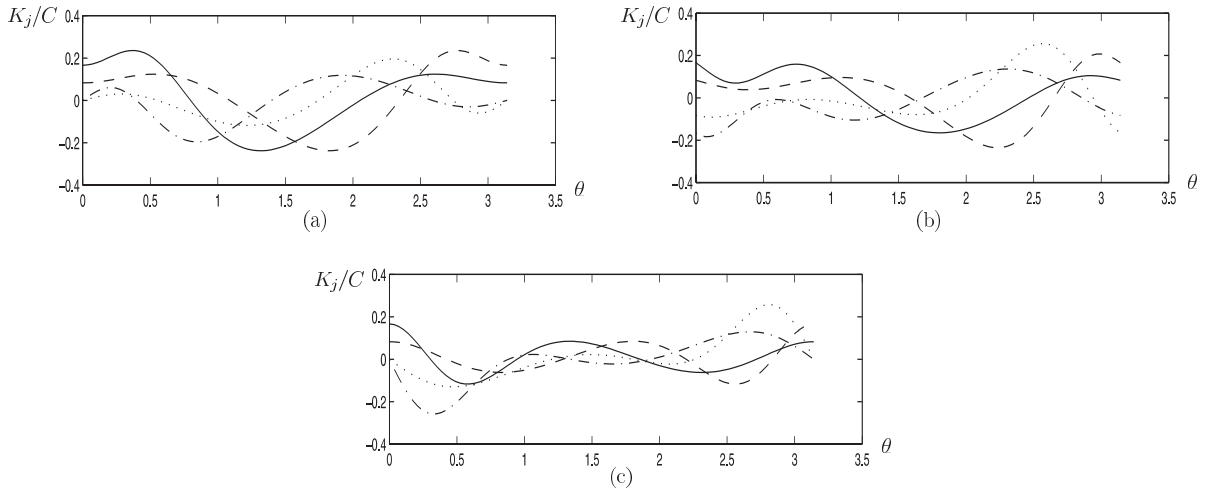


Fig. 3. Perturbation of the normalized stress-intensity factors  $C^{-1}K_j^\pm$  versus  $\theta$ . (—)  $C^{-1}K_I^+$ , (---)  $C^{-1}K_I^-$ , (· · ·)  $C^{-1}K_{II}^+$ , (· · · ·)  $C^{-1}K_{II}^-$ ; (a)  $\beta = 0$ , (b)  $\beta = \pi/4$ , and (c)  $\beta = \pi/2$ .

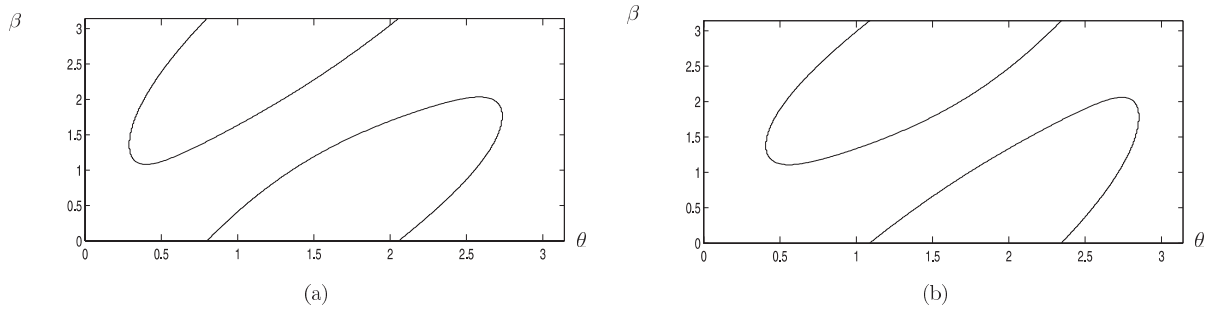


Fig. 4. Regions of local stability in the plane  $(\theta, \beta)$  for  $R/a = 3$ : (a)  $K_I^+$  and (b)  $K_I^-$ .

$$C = 5Ef T\alpha_T/[8(1 - v^2)],$$

and for the hexagonal lattice,

$$C = 3E(f - f^3/2)T\alpha_T/[4(1 - v^2)].$$

To characterize the local stability of the crack  $M$  (we say that it is locally stable if the increment of the stress-intensity factor  $K_I$  is negative, and unstable otherwise), we present Fig. 4, which shows the regions of stability on the plane  $(\theta, \beta)$ ; the calculations have been performed for the case when  $R/a = 3$ , where  $R = \sqrt{(x_1^{(0)})^2 + (x_2^{(0)})^2}$ . Inside the ellipsoidal regions in Fig. 4, we have the points of local stability, and all remaining points correspond to an unstable crack.

## 7. Conclusion

We have analysed a perturbation problem of the crack–defect interaction in the homogenized lattice structure. Explicit asymptotic formulae for the stress-intensity factors and for the crack deflection have

been derived, and the phenomenon of local stability was studied for a macro-crack in an inhomogeneous solid. The homogenization procedure is shown to be extremely efficient for the cases of cracks which are sufficiently large compared to the size of the lattice. The algorithm is used to compare different types of lattice structures and includes the cases of triangular, hexagonal and square lattices that are commonly used in design of catalytic monolith combustors.

### Acknowledgements

The work was supported by the UK Engineering and Physical Sciences Research Council (EPSRC), grant no. GR/K76634. The authors are grateful to the referees for the comments.

### References

Antipov, Y.A., Kolaczkowski, S.T., Movchan, A.B., Spence, A., 2000. Asymptotic analysis for cracks in a catalytic monolith combustor. *Int. J. Solids Struct.* 37, 1899–1930.

Chen, J.Y., Huang, Y., Ortiz, M., 1998. Fracture analysis of cellular materials: a strain gradient model. *J. Mech. Phys. Solids* 46, 789–828.

Cotterell, B., Rice, J.R., 1980. Slightly curved or kinked cracks. *Int. J. Fract.* 16, 155–169.

Gibson, L.J., Ashby, M.F., 1998. *Cellular Solids*. Pergamon Press, Oxford.

Gong, S.-X., Horii, H., 1989. General solution to the problem of micro-cracks near the tip of a main crack. *J. Mech. Phys. Solids* 37, 27–46.

Hayes, R.E., Kolaczkowski, S.T., 1997. *Introduction to Catalytic Combustion*. Gordon and Breach, New York.

Hori, M., Nemat-Nasser, S., 1987. Interacting micro-cracks near the tip in the process one of a macro-crack. *J. Mech. Phys. Solids* 35, 601–629.

Kolaczkowski, S.T., Lin, P., Movchan, A.B., Serkov, S.K., Spence, A., 1999. Thermal stress analysis and homogenization for catalytic combustor monoliths. *Eur. J. Appl. Math.* 10, 185–220.

Movchan, A.B., Nazarov, S.A., Polyakova, O.R., 1991. The quasi-static growth of a semi-infinite crack in a plane containing small defects, vol. 313. *C.R. Acad. Paris, Serie II*, pp. 1223–1228.

Movchan, A.B., Serkov, S.K., 1997. The Polya–Szegö matrices in asymptotic models of dipole composites. *Eur. J. Appl. Math.* 8, 595–621.

Rubinstein, A.A., 1986. Macro-crack–micro-defect interaction. *ASME J. Appl. Mech.* 53, 505–510.

Sedov, L.I., 1972. *A course in continuum mechanics*, vol. 4. Wolters-Noordhoff, Groningen.

Valentini, M., Serkov, S.K., Bigoni, D., Movchan, A.B., 1999. Crack propagation in a brittle elastic material with defects. *J. Appl. Mech.* 66, 79–86.